Using Landsat/TM Imagery to Estimate Nitrogen and Phosphorus Concentration in Taihu Lake, China

Article *in* IEEE Journal of Selected Topics in Applied Earth Observations and Remote Sensing · February 2012

DOI: 10.1109/JSTARS.2011.2174339

2 authors, including:

Jun Chen
Xi'an Jiaotong University
46 PUBLICATIONS **828** CITATIONS

IEEE JOURNAL OF

SELECTED TOPICS IN APPLIED EARTH OBSERVATIONS AND REMOTE SENSING

A PUBLICATION OF THE IEEE GEOSCIENCE AND REMOTE SENSING SOCIETY
AND THE IEEE COMMITTEE ON EARTH OBSERVATIONS

FEBRUARY 2012 VOLUME 5 NUMBER 1 IJSTHZ (ISSN 1939-1404)

SPECIAL ISSUE ON OPTICAL MULTI-ANGULAR DATA

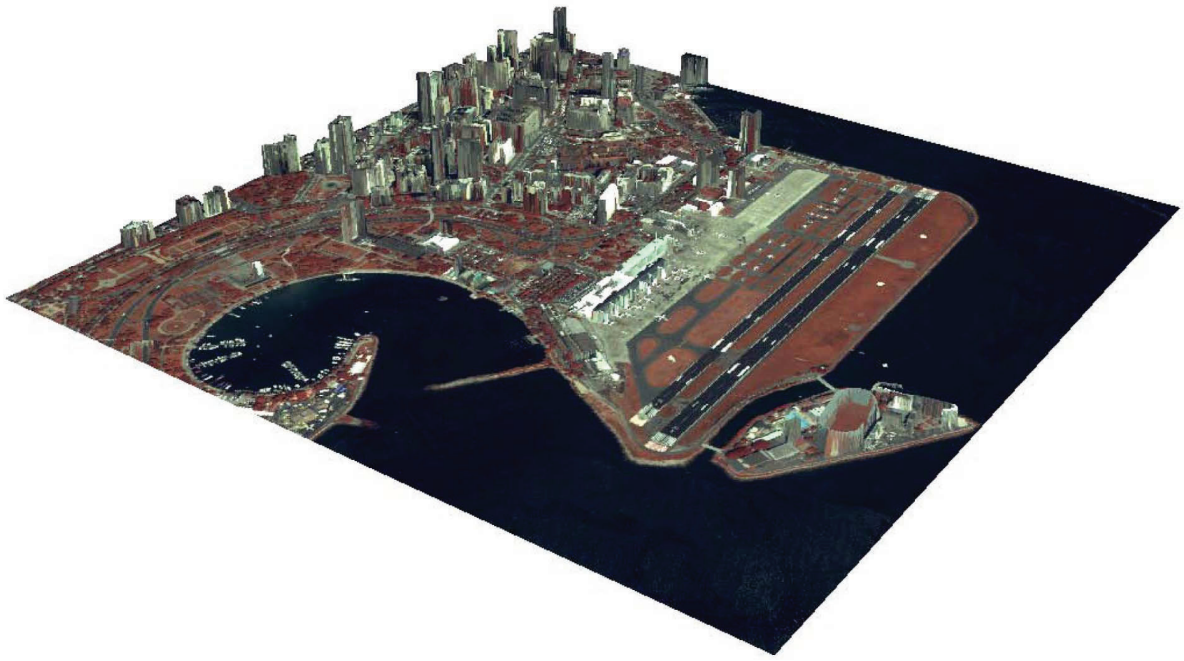

3D rendering representing the downtown of Rio de Janeiro retrieved using a WorldView-2 multi-angular sequence.

IEEE JOURNAL OF
SELECTED TOPICS IN APPLIED EARTH OBSERVATIONS AND REMOTE SENSING

A PUBLICATION OF THE IEEE GEOSCIENCE AND REMOTE SENSING SOCIETY AND THE IEEE COMMITTEE ON EARTH OBSERVATIONS

FEBRUARY 2012 VOLUME 5 NUMBER 1 IJSTHZ (ISSN 1939-1404)

SPECIAL ISSUE ON OPTICAL MULTIANGULAR DATA EXPLOITATION AND OUTCOME OF THE 2011 GRSS DATA FUSION CONTEST

Foreword to the Special Issue on Optical Multiangular Data Exploitation and Outcome of the 2011 GRSS Data Fusion Contest ..... *F. Pacifici and Q. Du* 3

Vegetation Structure Retrieval in Beech and Spruce Forests Using Spectrodirectional Satellite Data ..... *M. Schlerf and C. Atzberger* 8

Improving the Robustness of Cotton Status Characterisation by Radiative Transfer Model Inversion of Multi-Angular CHRIS/PROBA Data ..... *W. A. Dorigo* 18

Potential of Multi-Angular Data Derived From a Digital Aerial Frame Camera for Forest Classification ..... *T. Koukal and C. Atzberger* 30

Forest Canopy Cover and Height From MISR in Topographically Complex Southwestern US Landscapes Assessed With High Quality Reference Data ..... *M. Chopping, M. North, J. Chen, C. B. Schaaf, J. B. Blair, J. V. Martonchik, and M. A. Bull* 44

Performance Evaluation for 3-D City Model Generation of Six Different DSMs From Air- and Spaceborne Sensors ..... *B. Sirmacek, H. Taubenböck, P. Reinartz, and M. Ehlers* 59

Retrieval of the Height of Buildings From WorldView-2 Multi-Angular Imagery Using Attribute Filters and Geometric Invariant Moments ..... *G. A. Licciardi, A. Villa, M. Dalla Mura, L. Bruzzone, J. Chanussot, and J. A. Benediktsson* 71

Fast Surface Height Determination Using Multi-Angular WorldView-2 Ortho Ready Urban Scenes ..... *G. Lemoine, C. M. Bielski, and J. Syryczyński* 80

A Hybrid Approach for Building Extraction From Spaceborne Multi-Angular Optical Imagery ..... *A. Turlapaty, B. Gokaraju, Q. Du, N. H. Younan, and J. V. Aanstoos* 89

Improving Landsat ETM+ Urban Area Mapping via Spatial and Angular Fusion With MISR Multi-Angle Observations ..... *B. Huang, H. Zhang, and L. Yu* 101

An Operational Superresolution Approach for Multi-Temporal and Multi-Angle Remotely Sensed Imagery ..... *J. Ma, J. Cheung-Wai Chan, and F. Canters* 110

An Adjustable Pan-Sharpening Approach for IKONOS/QuickBird/GeoEye-1/WorldView-2 Imagery ..... *T.-M. Tu, C.-L. Hsu, P.-Y. Tu, and C.-H. Lee* 125

(Contents Continued on Page 2)

(Contents Continued from Page 1)

Automatic Moving Vehicles Information Extraction From Single-Pass WorldView-2 Imagery ..... *B. Salehi, Y. Zhang, and M. Zhong* 135
Object Tracking Using High Resolution Satellite Imagery ..... *L. Meng and J. P. Kerekes* 146

REGULAR PAPERS

Synthetic Aperture Radar Measurements of a Retreating Firn Line on a Temperate Icecap ..... *I. A. Brown* 153
Morphological Building/Shadow Index for Building Extraction From High-Resolution Imagery Over Urban Areas ..... *X. Huang and L. Zhang* 161
Simulation of Future Geostationary Ocean Color Images ..... *M. Lei, A. Minghelli-Roman, A. Bricaud, J. M. Froidefond, S. Mathieu, and P. Gouton* 173
Spatial Sub-Sampling Using Local Endmembers for Adapting OSP and SSEE for Large-Scale Hyperspectral Surveys ..... *D. Rogge, M. Bachmann, B. Rivard, and J. Feng* 183
A Fusion Approach to Retrieve Soil Moisture With SAR and Optical Data ..... *R. Prakash, D. Singh, and N. P. Pathak* 196
Interactive Spectral Band Discovery for Exploratory Visual Analysis of Satellite Images ..... *D. Bratasanu, I. Nedelcu, and M. Datcu* 207
Fusion of Textural and Spectral Information for Tree Crop and Other Agricultural Cover Mapping With Very-High Resolution Satellite Images ..... *A. A. Ursani, K. Kpalma, C. C. D. Lelong, and J. Ronsin* 225
Evidence of Atmospheric Brown Clouds Over India During the 2009 Drought Year ..... *P. R. C. Rahul, R. L. Bhawar, P. S. Salvekar, P. C. S. Devara, and J. H. Jiang* 236
A Source Apportionment Approach to Study the Evolution of Convective Cells: An Application to the Nowcasting of Convective Weather Systems ..... *B. P. Shukla and P. K. Pal* 242
FPGA Implementation of Abundance Estimation for Spectral Unmixing of Hyperspectral Data Using the Image Space Reconstruction Algorithm ..... *C. González, J. Resano, A. Plaza, and D. Mozos* 248
A Marker-Based Approach for the Automated Selection of a Single Segmentation From a Hierarchical Set of Image Segmentations ..... *Y. Tarabalka, J. C. Tilton, J. A. Benediktsson, and J. Chanussot* 262
Using Landsat/TM Imagery to Estimate Nitrogen and Phosphorus Concentration in Taihu Lake, China ..... *J. Chen and W. Quan* 273
Classification of Pansharpened Urban Satellite Images .... *F. Pálsson, J. R. Sveinsson, J. A. Benediktsson, and H. Aanæs* 281
Modeling Aboveground Biomass in Tropical Forests Using Multi-Frequency SAR Data—A Comparison of Methods ..... *S. Englhart, V. Keuck, and F. Siegert* 298
Night Thermal Gradient: A New Potential Tool for Earthquake Precursors Studies. An Application to the Seismic Area of L'Aquila (Central Italy) ..... *L. Piroddi and G. Ranieri* 307
Combination of Anomaly Algorithms and Image Features for Explosive Hazard Detection in Forward Looking Infrared Imagery ..... *D. T. Anderson, K. E. Stone, J. M. Keller, and C. J. Spain* 313
Estimation on Scale Error of SSC Retrieval Model Based on Scale Expansion Method ..... *J. Chen and W. Quan* 324
Multi-Modal Change Detection, Application to the Detection of Flooded Areas: Outcome of the 2009–2010 Data Fusion Contest ..... *N. Longbotham, F. Pacifici, T. Glenn, A. Zare, M. Volpi, D. Tuia, E. Christophe, J. Michel, J. Inglada, J. Chanussot, and Q. Du* 331

Using Landsat/TM Imagery to Estimate Nitrogen and Phosphorus Concentration in Taihu Lake, China

Jun Chen and Wenting Quan

***Abstract*—In this study, we evaluate the benefits of the use of broad-band reflectance data from remote-sensing imagery for improving point prediction of N (Nitrogen) and PC (Phosphorus Concentration) in lakes. The algorithms were calibrated and validated by in situ measurements, collected on 27 and 28 October, 2003, in Taihu Lake, China. Both two algorithms produced well performance in estimating NC and PC in Taihu Lake, but the PC retrieval model had a superior performance to NC retrieval model. The RE (Relative Error) of the PC and NC retrieval models were 11.7% and 35.6%, respectively. According to no more than 30% accuracy requirements of water quality estimation for remote-sensing technology, the accuracy of PC retrieval model is more acceptable than the NC retrieval mode's. Finally, the PC and NC were estimated from Landsat/TM imagery, collected on 28 October, 2003. The retrieval results showed that the NC and PC were higher in the south, east and center of the lake ($>$18 mg/l and $>$2 mg/l for NC and PC, respectively) and lower in the west and north of the lake ($<$18 mg/l and $<$2 mg/l for NC and PC, respectively). Although it was a special case study of this paper, the modeling procedures of NC and PC estimation algorithms could give us the implication when we used the remote-sensing technology to estimate the NC and PC from similar or dissimilar aquatic environments**

***Index Terms*—Nitrogen concentration, phosphorus concentration, remote sensing, Taihu Lake.**

I. Introduction

LAKES are valuable water resources, which could be used for fishing, transport, agriculture, industry and tourism [1].

However, over the past 50 years, as is widely known, most aquatic environments have changed under the increasing pressure of human activities. For example, changes in water use, loading of municipal and industrial sewage into aquatic environments and overuse of organic and inorganic fertilizers resulted in water pollution [2]. These changes have influenced the substance and energy balance in the aquatic ecosystem. Further, the lifestyles of human society have been impacted by the hazardous consequences that were caused by the changes in the ecological environment.

N and P are important essential micronutrients for algae. They stimulate the over-production of algae, and lead to undesirable states of eutrophication in lakes and reservoirs, if the NC and PC exceed the accepted concentration ranges of a healthy water environmental ecological system [3]. Therefore it was important to monitor the NC and PC on a large scale. However, because of the lack of suitable well-established methods, a spatial overview of NC and PC has been rarely measured on a large scale [4]. Although traditional NC and PC monitoring approaches give accurate measurements, they are costly, time consuming and often require direct contact with the body of water from which a sample may be taken; this may result in affecting the NC and PC of water samples. Additionally, some regions are often inaccessible or logistically difficult for field-based monitoring methods. In comparison, remote-sensing imagery can span across the extent of large inland lakes and validate in situ nutrient concentration estimates measurements, as well as to interpolate or extrapolate, predicting NC and PC to areas that are not sampled. This is needed for better regional monitoring and assessment the lake-wide stratification effects, water movement and other ecosystem-interaction effects on lake water quality.

The development of remote-sensing technology has the potential to solve the problems caused by the traditional monitoring approach. Remote-sensing provides a synoptic solution for detecting water elements over a large spatial area. Although the NC and PC estimated by remote-sensing approaches has been widely used to estimate the NC and PC in plants [5]–[8], there is still little literature with regard to estimate NC and PC from remote sensing. As described by Hood *et al.* [9], two unique optical characteristics of chlorophyll-a (chl-a), absorption and fluorescence, are strongly related with the NC and PC. Lately, Hanson *et al.* [10] also proves the points regarding that the fluorescence of chl-a would be influenced by the NC and PC. Additionally, previous studies reveal that suspended sediment concentration (SSC), chl-a and colored dissolved organic matters (CDOM) are important substance sources of the N and P elements [3], [11]. As delineated by Cavalli *et al.* [12], Hadjimitsis *et al.* [13], and Volpe *et al.* [14], it is now feasible to detect and estimate chl-a, SSC and CDOM concentration using welling radiance measurements from water color sensors such as Landsat Thematic Mapper (Landsat/TM), which would provide possible to estimate NC and PC from remote sensing.

Landsat/TM is cheap and has very long times series of archived data which can provide insight about historical events or developments in an area and can therefore be utilized for

Manuscript received July 07, 2011; revised September 22, 2011; accepted October 19, 2011. Date of publication December 07, 2011; date of current version February 29, 2012. This work was supported by the open fund of China Ministry of Land and Resource of the Key Laboratory of Marine Hydrocarbon Resources and Environment Geology (MRE201109) and The Program of the China National Great Geology Survey (GZH200900504).

J. Chen is with the the Key Laboratory of Marine Hydrocarbon Resources and Environmental Geology, Qingdao Institute of Marine Geology, Qingdao, Shandong, China (corresponding author, e-mail:cjun@cgs.cn).

W. Quan is with Shanxi Remote Sensing Information Center Agriculture, China (e-mail: cloudy1112@gmail.com).

Color versions of one or more of the figures in this paper are available online at http://ieeexplore.ieee.org.

Digital Object Identifier 10.1109/JSTARS.2011.2174339

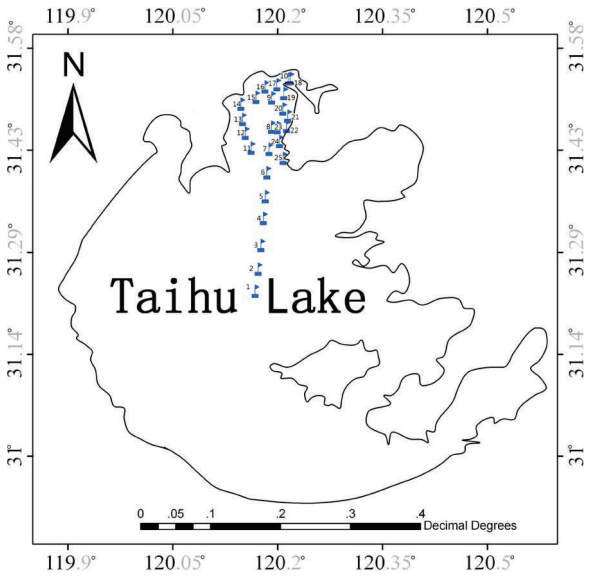

Fig. 1. The Taihu Lake (The blue flags were sampling stations, and the Arabic numerals were serial number of experimental stations).

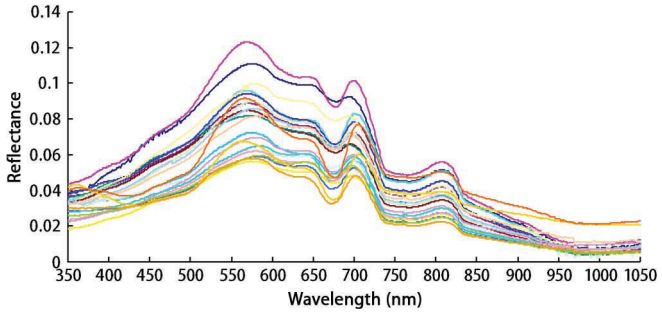

Fig. 2. Spectral curves used to calibrate and validate the remote sensing model in this study.

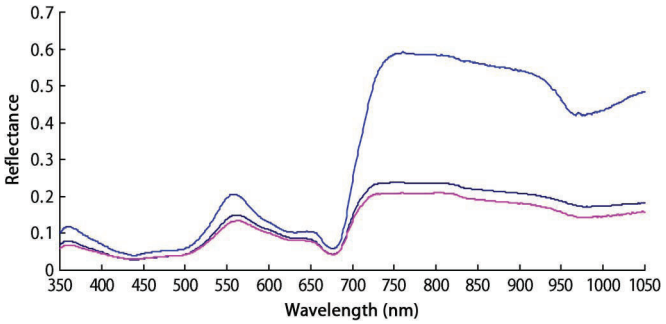

Fig. 3. Spectral curves with high value in infrared wavelength.

monitoring purposes. Previous studies show that Landsat has proven its capabilities to yield satisfactory results in lake water studies [15]–[17]. The idea, then, is to use relationship between nutrients concentration and bio-optical matters (chl-a, SSC and CDOM) as the basis to estimate NC and PC from the remote sensing system of Landsat/TM. However, because of the lack of suitable well-established remote-sensing retrieval methods, there is little consensus on the best NC and PC retrieval algorithms for reflectance of Landsat/TM imagery in terms of its accuracy and reliability. The main objectives of this study were: (1) to develop an empirical retrieval algorithm for estimating NC and PC from Landsat/TM imagery, (2) to calibrate and validate the remote-sensing retrieval models, collected on 27 and 28 October, 2003, in Taihu Lake, and (3) to estimate the NC and PC from Landsat/TM imagery in Taihu Lake, China.

II. Study Area

Taihu Lake is a typical inland water body, located between $119°54'\mathrm{E}$ and $120°36'\mathrm{E}$ and between $30°56'\mathrm{N}$ and $31°33'\mathrm{N}$ (Fig. 1). The lake had an average water depth of 1.89 m. Located on the northern border of the subtropical broad-leaved forest region, it belongs to the southeast monsoon climate area. The rainy season occurs in summer. The annual average air temperature of this region is 14.9–16.2°C. The annual mean precipitation was 1000–1400 mm and the annual mean runoff into the lake is 4100 Mm^3 [18].

Taihu Lake is a very large shallow lake. Its total P and total N concentration varied between 0.08 and 0.12 mg/l, with an average of 0.09 mg/l, and between 1.84 mg/l and 2.22 mg/l, with an average of 1.99 mg/l, respectively [19]. There are significant horizontal differences in water quality and ecosystem structure in Taihu Lake. The east and the south parts of the lake are phytoplankton-dominated with relatively worse water quality, while the north and the west parts are macrophyte-dominated with relatively better water quality. The dominant species in the phytoplankton-dominated area of Lake Taihu is *Microcystis spp*.

III. Materials and Methods

A. Data Used

The data used in this study was collected on 27 and 28 October, 2003. It included 25 samples of hyperspectral reflectance, SSC, chl-a, CDOM, NC and PC. The spectral curves at No. 22, No. 23 and No. 25 experimental stations had a very high infrared wavelength (Fig. 2). The spectral curves of those three stations appeared to be non-water spectral, whose spectral reflectance at red regions was higher than near-infrared regions (Fig. 3). In general, the spectral reflectance of water bodies at red regions was lower than that at near-infrared regions. Thus, the data of these three experimental stations was not used to calibrate and validate the NC and PC retrieval algorithms in this study.

The data was classed into two groups, one as model calibration data (16 samples, about 70% of total samples) and the other as model validation data (6 samples, about 30% of total samples). To make sure that the NC or PC of validation dataset can represent the concentration range of the data collected in Taihu Lake, on October 27–28, 2003, the data was ranged in descending order by values of NC OR PC, and the validation data of NC OR PC was selected once every three stations from the sorting results as given above. The descriptive statistics of the validation data and calibration data were shown in Tables I–IV.

The synchronous Landsat-5 imagery is collected when the fieldwork was carried out on 28 October, 2003. The Landsat/TM, a NASA satellite launched on 1 March 1984, was selected for acquiring broad-band reflectance data (Landsat-5 imageries with $\mathrm{path} = 119$ and $\mathrm{row} = 38$). The Landsat/TM included the following optical bands: blue—green (TM1: 450–520 nm), green (TM2: 520–600 nm), red (TM3: 630–690 nm), near infrared (TM4: 760–900 nm), short infrared

TABLE I
DESCRIPTIVE STATISTICS OF DATASET FOR CALIBRATING THE NITROGEN RETRIEVAL MODEL

	Min	Max	Median	Average	STDEV
SSC (mg/l)	19.64	78.56	41.68	46.33	21.47
CDOM (mg/l)	4.86	7.79	5.56	5.93	0.94
Chl-a (μg/l)	2.2	47.46	18.00	20.57	13.27
NC (mg/l)	0.98	6.29	2.71	2.93	1.53
PC (mg/l)	0.19	0.33	0.21	0.22	0.03

TABLE II
DESCRIPTIVE STATISTICS OF DATASET FOR VALIDATING THE NITROGEN RETRIEVAL MODEL

	Min	Max	Median	Average	STDEV
SSC (mg/l)	27.32	65.56	55.54	51.39	14.93
CDOM (mg/l)	4.63	11.29	6.71	7.76	2.82
Chl-a (μg/l)	7.70	123.26	21.07	46.84	48.28
NC (mg/l)	1.17	5.35	2.78	3.01	1.53
PC (mg/l)	0.18	0.35	0.21	0.24	0.07

TABLE III
DESCRIPTIVE STATISTICS OF DATASET FOR CALIBRATING THE PHOSPHORUS RETRIEVAL MODEL

	Min	Max	Median	Average	STDEV
SSC (mg/l)	19.64	78.56	39.48	44.87	20.06
CDOM (mg/l)	4.86	11.16	5.87	6.30	1.59
Chl-a (μg/l)	2.2	123.26	18.00	27.03	28.89
NC (mg/l)	0.98	6.29	2.75	3.14	1.63
PC (mg/l)	0.18	0.35	0.21	0.22	0.05

TABLE IV
DESCRIPTIVE STATISTICS OF DATASET FOR VALIDATING THE PHOSPHORUS RETRIEVAL MODEL

	Min	Max	Median	Average	STDEV
SSC (mg/l)	27.32	74.76	55.54	55.28	18.06
CDOM (mg/l)	4.63	11.29	5.98	6.78	2.39
Chl-a (μg/l)	7.70	91.51	18.19	29.59	30.85
NC (mg/l)	1.33	4.08	2.11	2.46	1.01
PC (mg/l)	0.19	0.31	0.21	0.22	0.04

(TM7: 2080–2350 nm) and the thermal infrared band (TM6: 10400–12500 nm).

B. Field Measurements

In situ measurements were carried out in Taihu Lake on 27 and 28 October, 2003. The distribution of in situ sampling points is given in Fig. 1 and the spectral curves of the in situ measurements are shown in Fig. 2. At each station, hyperspectral reflectance measurements were taken from a boat using. The reflectance was measured with a spectroradiometer with 25° fiber-optic, covering the spectral domain of 350 nm–2500 nm (Spectral Devices, Boulder, CO, ASD). Data were collected in the range of 350–2500 nm, with a spectral resolution of 3 nm (full-width-at-half-maximum, FWHM) and a 1.4 nm sampling interval for the 350 nm–1050 nm spectral range [20]. During the measurements, the tip of the optical fiber was kept just below the water surface by means of a 3 m long, hand-held black pole. In order to effectively avoid the interference of the ship with the water and the direct solar radiation, the optical fiber was positioned at an angle of 90–135° with the plane of the incident radiation away from the sun. The view of the water surface was controlled between 30–45° with the aplomb direction. Immediately after measuring the water radiance, the spectroradiometer was rotated upwards by 90–120° to measure skylight. The view zenith angle in this measurement was kept the same as that in measuring water radiance [21].

Hyperspectral reflectance was calculated as follows:

$$R_{\mathrm{rs}}(\lambda) = \frac{L_{\mathrm{w}}(\lambda)}{E_{\mathrm{d}}^{0+}(\lambda)} \tag{1}$$

where $L_{\mathrm{w}}(\lambda)$ is the water-leaving radiance, $E_{\mathrm{d}}^{0+}(\lambda)$ is the total incident radiant flux of the water surface and $R_{\mathrm{rs}}(\lambda)$ is the remote-sensing reflectance. $L_{\mathrm{w}}(\lambda)$ and$E_{\mathrm{d}}^{0+}(\lambda)$ in (1) are further calculated as follows:

$$L_{\mathrm{w}}(\lambda) = L_{\mathrm{sw}}(\lambda) - rL_{\mathrm{sky}}(\lambda), \tag{2}$$

$$E_{\mathrm{d}}^{0+}(\lambda) = \frac{\pi L_{\mathrm{p}}(\lambda)}{\rho_{\mathrm{p}}(\lambda)} \tag{3}$$

where $L_{\mathrm{sw}}(\lambda)$ denotes the total radiance received from the water surface; $L_{\mathrm{sky}}(\lambda)$ presents the diffused radiation of the sky, which contained no information on water properties, and hence had to be eliminated; r refers to the reflectance of the skylight at the air-water interface, the value of which depended upon the solar azimuth, measurement geometry, wind speed and surface roughness; $L_{\mathrm{p}}(\lambda)$ is the radiance of the gray board; $\rho_{\mathrm{p}}(\lambda)$ is the reflectance of the gray board.

C. Laboratory Measurements

Water samples were collected immediately after the radiance measurements. At each station a standard set of water quality parameters was measured. These included chl-a concentration, CDOM, SSC, NC and PC. The surface water samples were collected at a depth of 0.5 m below the water-air surface. After sampling, water samples in bottles were conserved at a low temperature and sent for laboratory analysis in the afternoon.

The laboratory analyses were carried out within 24 h following sample collection. Water samples for CDOM measurements were immediately filtered through precombusted GF/F filters (0.7 μm pore size) before future treatment. The CDOM was quantified by fluorescence detection method advised by Mueller & Fargion [21]. The chl-a concentration were extracted and measured with 90% acetone in accordance with the Ocean Optical Protocols of NASA [21]. The total suspended sediment concentrations, broken down into mineral (SSC) and organic fractions, were measured gravimetrically on pre-weighed, washed and combusted glass-fiber filters (47 mm diameter, 0.7 μm pore size). Sufficient water was filtered (up to 3 L) to enable consistency in the weight determination of the particulate matter. Samples were rinsed with distilled water to remove all dissolved salts and stored frozen until processed. Filters were dried overnight at 70°C and then combusted at 500°C for three hours for the determination of SSC. The NC was measured by the second derivative method after a persulfate digestion [22]. PC was determined using the ascorbic acid method after persulfate oxidation [23].

D. Atmospheric Correction

In case I and case II waters, the component of the measured radiance which carries information about the water quality parameters, the radiance backscattered off the water surface and

transmitted to the top of the atmosphere, is at most 10% of the measured radiance in the blue and typically much smaller in the green regions. The rest of the signal is comprised of radiance reflected from the atmosphere and the water surface. Thus the water-leaving radiance must be extracted from the total radiance received by sensors—a process referred as atmospheric correction [24].

In the past, a variety of algorithms were developed for retrieving the water-leaving radiance from remote-sensing imagery, including the empirical and radiance transfer models [25], [26]. Most of these algorithms took advantage of the optical properties of water at near-infrared bands. The widely applied approach was the DPA (Dark Pixels Algorithm), which assumed that there were dark pixels whose water-leaving radiance is assumed to be zero at the near-infrared bands in the imagery[27], [28]. However, such an atmospheric correction method was not available for such turbid water bodies as Taihu Lake, due to the detrital material scattering at the near-infrared wavelength [29]. Additionally, aerosol content was non-isotropic above the inland lake. As a result, the atmospheric correction of the clear water bodies developed by Gordon and Clark [28] was not applicable for retrieving the water-leaving reflectance from remote-sensing imagery in Case II water bodies. Considering the in situ measurements were carried out when the Landsat/TM satellite passed over Taihu Lake, China, the study used the water-leaving reflectance retrieval algorithm, developed by Chen *et al.* [30], to remove the atmospheric effects. Space dose not permit a full review of this atmospheric correction algorithm here, instead, the reader is referred to our previous research [30].

E. Relationships Between Nutrient Elements and Bio-Optical Matters

Eutrophication of nature waters produced by an enhanced supply of nutrients has been recognized in recent years as a serious environmental problem, and required the development of simple procedures and screening models for predicting this phenomenon [31]. In freshwater situations, the relationship between the loading of nutrient elements (such as N and P) and mean concentration of water quality parameters, SSC, CDOM and chl-a, have been demonstrated as a reliable parameter for predicting eutrophication [11]. However, because coastal environments and turbid inland waters were more rapidly flushed than freshwater in a similar volume, it became difficult to further understand the dynamic relationship between the supply of nutrient matters and the concentration of water quality parameters in those water bodies [32].

Fig. 4 showed the matters cycle of the aquatic ecosystem. Fig. 4 shows that the phytoplankton consumed nutrients from its confining waters and in the presence of subsurface sunlight synthesized these nutrients into organic matter. When the phytoplankton cells decomposed in the water, the organic matter was chemically transformed, through microbial action on timescales of days to weeks, to carbon dioxide and inorganic N and phosphorous compounds. The decomposition process resulted in the creation of a variety of complex polymers generally referred to as the humic substances. These humic substances comprised both water-soluble and water-insoluble fractions. The water-soluble fraction comprised dissolved organic carbon in the form of humic acid, which would transform to CDOM through the temperature-dependent Maillard reaction; the water-insoluble fraction was an important component of the suspended matters [33]. Therefore, the NC and PC in water bodies were closely related to the concentration of water quality parameters. It is well known that the bio-optical properties of water columns are mainly depended on the concentrations of chl-a, CDOM and SSC [14], [29], [37]. As a result, the NC and PC would greatly indirectly effects on the bio-optical properties of water columns, which can be used to illuminate the reason why we can use the remote sensing technology to estimate the NC and PC from inland waters. In our previously study, we used an experimental data of this study to construct the relationships between the concentration of nutrient matters and the concentration of water quality parameters [34]:

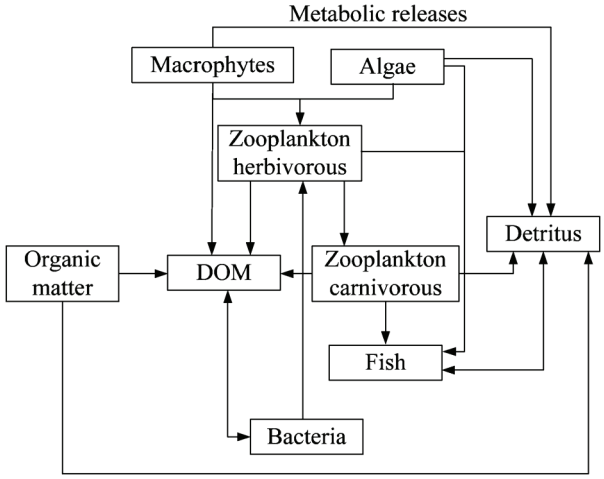

Fig. 4. Matters cycle in the aquatic ecosystem.

$$C_{\mathrm{P}} = 0.25C_{\mathrm{CDOM}} + 0.069, \quad n = 25 \tag{4}$$

$$C_{\mathrm{N}} = -0.009C_{\mathrm{Chla}} - 0.039C_{\mathrm{SSC}} + 0.48C_{\mathrm{CDOM}} + 1.963,$$
$$R^2 = 0.676, \quad n = 25 \tag{5}$$

$$C_{\mathrm{P}} = 0.1502e^{0.1502C_{\mathrm{N}}}, \quad R^2 = 0.705, \quad n = 25 \tag{6}$$

where C_{CDOM}, C_{Chla}, C_{SSC}, C_{P}, and C_{N} were the concentration of CDOM, SSC, chl-a, NP, and NC, respectively. Eq. (4)–(6) showed that the PC had the higher regression coefficient than NC. In general, the PC was considered as the main limiting nutrient in the ecosytems of inland lakes, and its concentration was used to predict the total biomass of phytoplankton [35]. The higher regression coefficient of PC also revealed that Taihu Lake was a P-limiting lake; this was in agreement with the results of the study carried out by Zhai *et al.* [36].

F. Nutrient Elements Concentration Retrieval Algorithm

Considerable progress has been made to develop a general model of ecosystem operation to understand how phytoplankton in aquatic environments interacted with regional and general nutrients circulation models [38]. Ecosystem models were the ties that combined together the phytoplankton, ecosystem dynamic and functions simulation, photosynthesis and nutrients dynamics [39]. As the key parameters of ecosystem models,

the spatial information about the NC and PC distribution appeared significantly important, to fully understand the physical and biological mechanism of the substance and emerge cycle in an aquatic ecosystem. Although traditional point sampling methods had the ability to give accurate measurements, they were time-consuming and it was difficult to give a lake-scale overview of the study area. The remote-sensing technology had the potential to solve these problems.

The three invisible bands and one near-infrared band of Landsat/TM imagery were in the spectral range where light passed through the water, providing some information about its quality concentration, and were usually used to estimate the concentration of water quality parameters. According to the literature [29], [40], TM1 was relatively low due to the combined effects of absorption by the CDOM, tripton and phytoplankton pigments. A local maximum in reflectance was found at TM2, which was caused by a local minimum in the combined effects of the low phytoplankton pigment absorption efficiency and lower CDOM and tripton absorption. A clear reflectance minimum was located at TM3, which was the in vivo chlorophyll-a maximum absorption peak. Beyond 680 nm, the reflectance increased significantly and reached a maximum at 706 nm, which could be used for interpretation of the signal due to the natural phytoplankton fluorescence; however the Landsat/TM did not have bands in this area.

The spectral curves as shown in Fig. 3 revealed that the reflectance in the blue range (400–500 nm) was relatively low due to the high absorption of water quality parameters. The reflectance in the green range (500–600 nm) and the red region (600–700 nm) was the primary and the secondary reflectance peak, respectively, formed by the scattering of the suspended sediment and low absorption coefficient of CDOM and chlorophyll-a pigment. Due to the high absorption of water bodies at long wavelength, the reflectance at near-infrared bands was low. Additionally, the reflectance in the blue region of the visible spectrum decreased at a rate nearly equivalent to that of the reflectance elevation in the green and far-infrared regions [41]. According to Fig. 4, it was found that the providing of NC and PC limited the productions of phytoplankton, which affected the productions of detritus, zooplankton, organic matter, DOM, and so on in water environmental ecological system. The N and P elements were contained in organic matter, detritus, DOM, algae, and so on. Additionally, the SSC, chl-a, and CDOM was the mainly substance sources of dissolved N and P elements [32]. As a result, owing to the close relationships between the concentration of nutrient elements and the concentration of water quality parameters ((4) and (5)), it was reasonable to suppose that the variation of concentration of nutrient elements would directly or indirectly lead to the changes of the spectral characteristics of water bodies. In general, the spectral reflectance varied with the changes of chl-a, CDOM, and SSC at Landsat imagery of TM1, TM2, TM3, and TM4 [27], [29]. In this way, the relationships between the concentration of nutrient elements and the Landsat/TM reflectance could be assumed as follows:

$$C_{\mathrm{N}} = f\left(R_{\mathrm{TM1}}, R_{\mathrm{TM2}}, R_{\mathrm{TM3}}, R_{\mathrm{TM4}}\right) \tag{7}$$

$$C_{\mathrm{P}} = g\left(R_{\mathrm{TM1}}, R_{\mathrm{TM2}}, R_{\mathrm{TM3}}, R_{\mathrm{TM4}}\right) \tag{8}$$

where $f()$ and $g()$ are the NC and PC retrieval model, respectively. R_{TM1}, R_{TM2}, R_{TM3}, and R_{TM4} are remote-sensing reflectance at TM1, TM2, TM3, and TM4, respectively.

G. Accuracy Assessment

In this study, the STDEV (Standard Deviation) is used an indicator of the accuracy. The formula of STDEV is as follows:

$$STDEV = \sqrt{\frac{\sum \left(S_{\mathrm{P}} - S_{\mathrm{T}}\right)^2}{N}} \tag{9}$$

where S_{P} is the predicated value of a model. S_{T} is truth of S_{P}. In most cases, it's hard to obtain the S_{T} of S_{P}, and the S_{T} generally takes place to S_{M} (Value of in situ measurement) or S_{A} (Average value of S_{M} or S_{P}).

The RE (Relative Error) between predicted values and these in situ measurements is as follows:

$$RE = \frac{STDEV}{S_{mean}} \times 100\% \tag{10}$$

The methods of accuracy assessment based on STDEV and RE can reveal the accuracy of the whole dataset. It is a comprehensive indicator, so it is unable to illuminate the level of accuracy at a given concentration.

IV. Results and Discussion

A. Model Calibration

In this paper, empirical models were used to construct the NC and PC retrieval model. To match the bandwidth of Landsat/TM, the ASD measurements, remote sensing reflectance, were aggregated using the Landsat/TM sensor spectral response functions before model calibration [42]. The calibration data was used to calibrate the empirical NC and PC retrieval models. All of these common empirical models, such as linear model, exponential model, logarithmic model, etc., were tested to determine the relationships between the PC, NC and remote-sensing parameters (such as reflectance, multi-bands linear combination, and bands ratio at TM1, TM2, TM3, and TM4). The model calibration results are shown in (11) and (12), respectively. According to the calibration results, it was found that the regression coefficients, R^2, of the NC retrieval model and the PC retrieval model were 0.24 and 0.63, respectively. The R^2 of the PC retrieval model was much higher than that of the NC retrieval model, which showed that the water color was more significantly affected by PC than by NC in P-limiting lakes of Taihu, China.

$$\begin{aligned} C_{\mathrm{N}} = & -275.26R_{\mathrm{TM1}} - 6.85R_{\mathrm{TM2}} + 224.43R_{\mathrm{TM3}} \\ & + 7.86R_{\mathrm{TM4}} + 3.48 \\ R^2 = & 0.24, \quad n = 16 \end{aligned} \tag{11}$$

$$\begin{aligned} C_{\mathrm{P}} = & -10.11R_{\mathrm{TM1}} + 0.85R_{\mathrm{TM2}} + 7.34R_{\mathrm{TM3}} + 2.04R_{\mathrm{TM4}} \\ & + 0.17 \\ R^2 = & 0.63, \quad n = 16 \end{aligned} \tag{12}$$

TABLE V
MODEL VALIDATION RESULTS OF NC RETRIEVAL MODEL (MG/L). THE SNE WAS THE SERIAL NUMBER OF EXPERIMENTAL STATIONS, AS SHOWN IN FIG. 1

SNE	Fieldworks	Predictions	STDEV	RE
4	1.910	3.185	-1.275	66.8%
9	1.170	2.378	-1.208	103.2%
11	2.320	2.772	-0.452	19.5%
20	3.240	3.116	0.124	3.8%
21	4.080	4.648	-0.568	13.9%
24	5.350	5.000	0.359	6.5%
Average	3.010	3.516	-0.505	35.6%

TABLE VI
MODEL VALIDATION RESULTS OF PC RETRIEVAL MODEL (mg/l)

SNE	Fieldworks	Predictions	STDEV	RE
4	0.195	0.257	-0.062	32.0%
6	0.204	0.175	0.029	14.1%
8	0.214	0.218	-0.004	1.8%
13	0.191	0.211	-0.020	10.7%
20	0.225	0.226	-0.001	0.3%
21	0.305	0.270	0.035	11.3%
Average	0.222	0.226	-0.004	11.7%

B. Model Validation

In order to access the accuracy of the NC and PC retrieval models, the model validation data was used to calculate the STDEV between the concentration of field and model predictions. Table V and Table VI showed the accuracy describing information about NC and PC retrieval model, respectively. According to Table V, Table VI, it was found showed that the RE of the PC and NC retrieval models were 11.7% and 35.6%, respectively. According to no more than 30% accuracy requirements of water quality estimation for remote-sensing technology [14], [40], the accuracy of PC retrieval model is more acceptable than the NC retrieval mode's. Additionally, the average error of the two retrieval models was lower than zero, which showed that nutrient concentration was overestimated by those two retrieval models.

C. Nutrient Elements Concentration Retrieval From Landsat/TM Imagery

The atmospheric correction algorithm developed in our previous works [43] was used to remove the atmospheric effects from Landsat/TM imageries. The detail information about the performance of atmospheric correction algorithm can be found at reference [43]. For simplicity, we would not repeatedly introduce the atmospheric correction results here.

Eq. (11) and (12) were used to estimate the NC and PC, respectively, from Landsat/TM imagery. Fig. 5 and Fig. 6, respectively, showed the NC and PC retrieved from Landsat/TM imagery in this study. According to Fig. 5, it was found that the NC was higher in the south, east and center of the lake (greater than 18 mg/l), and lower in the west and north of the lake (less than 18 mg/l). Fig. 6 showed that the PC was higher in the south, east and center of the lake (greater than 2 mg/l), and lower in the north and west of the lake (less than 2 mg/l). According to the results of the Zhai *et al.* study [36], it was found that the east and the south parts of the lake were phytoplankton-dominated with relatively worse water quality, while the north and the west

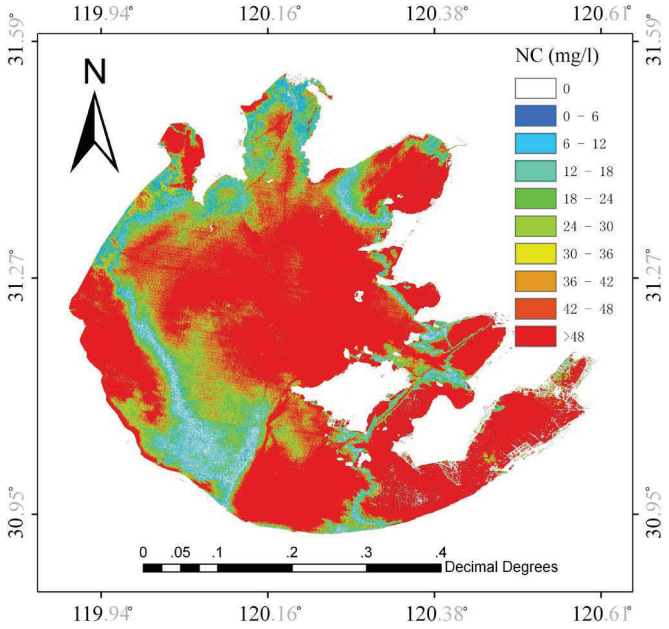

Fig. 5. Distribution of nitrogen concentration in Taihu Lake.

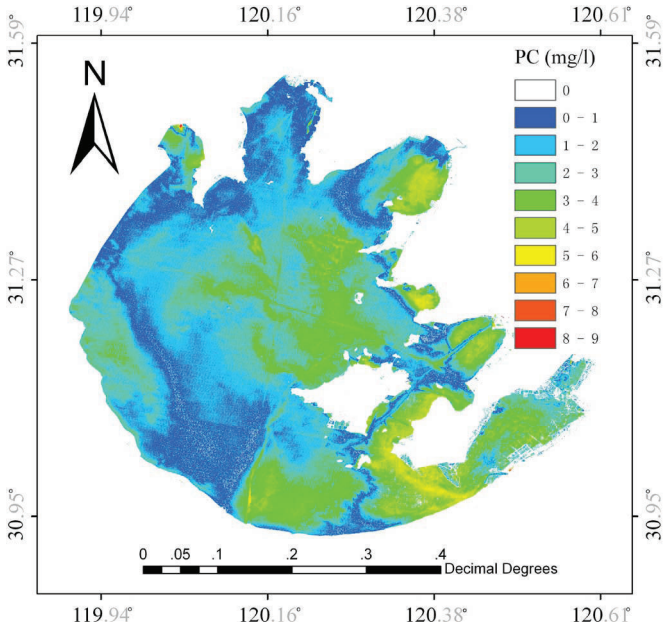

Fig. 6. Distribution of phosphorus concentration in Taihu Lake.

parts were macrophyte-dominated with relatively better water quality. The distribution patterns of PC and NC supported the study results of Zhai *et al.* [36].

The PC and total NC varied between 0.08 mg/l and 0.12 mg/l with an average of 0.09 mg/l and between 1.84 mg/l and 2.22 mg/l with an average of 1.99 mg/l, respectively [36]. By comparison, the NC and PC were greatly overestimated by the remote-sensing approach. The problems can be divided mainly into two groups: (1) the low accuracy of the retrieval model, and (2) the influence of atmospheric correction. The NC and PC indirectly influenced the colors of water bodies. As a result, the component of the measured radiance that carried information about the PC and NC was very small, which would lead

to the bad inversion results of those two water quality parameters (the R^2 of the NC and the PC retrieval models were 0.24 and 0.63, respectively). Additionally, the component of the measured radiance that carried information about the concentration of water quality parameters, backscattered off the water surface and transmitted to the top of the atmosphere, was at most 20% in the blue and typically much smaller in the green and near-infrared bands [27], [28]. The weak signal of water-leaving reflectance increased the difficulty to remove the atmospheric influences, which further decreased the accuracy for estimating the nutrient concentration from satellite imagery.

V. Conclusions

NC and PC were the important parameters when using dynamic models to predict the eutrophication status of coastal and inland waters. The current study characterized the spatial variability of two important water quality parameters—NC and PC—by field-measured spectral and remote-sensing reflectance in the Taihu Lake, China. The influences on Landsat/TM imagery were removed by the synchronized reflectance collected at 28 Oct, 2003. The methods of mapping the NC and PC were based on the empirical relationships between NC and reflectance at Landsat/TM bands. According to this study, it the following conclusions could be obtained:

1) The N and P were the nutrients necessary for the growth of the algae. The nutrient cycle showed that the algae consumed N and P from their confining waters, and in the presence of subsurface sunlight synthesized these nutrients into organic matter. When the phytoplankton cells decomposed into the water, the organic matter was chemically transformed, through microbial action to carbon dioxide, CDOM, suspended matters, inorganic N and phosphorous compounds. Accordingly, the NC and PC were closely related to the concentration of SSC, CDOM and chl-a. The regression analysis results showed that the correlation coefficients were 0.898 for the relationship between PC and the concentration of water quality parameters and 0.646 for the relationship between NC and the concentration of water quality parameters, respectively.
2) Although the water optical properties were not directly influenced by the fluctuations of NC and PC, the NC and PC were closely related to the concentration of SSC, chl-a and CDOM. According to the calibration results, it was found that the regression coefficient, R^2, of the NC retrieval model and the PC retrieval model was 0.24 and 0.63, respectively. The R2 of the PC retrieval model was much higher than that of the NC retrieval model, which showed that the water color was more significantly affected by PC than by NC in the P-limiting lake of Taihu, China. Additionally, the model-validated results showed that the RE of the PC and NC retrieval models were 11.7% and 35.6%, respectively. According to no more than 30% accuracy requirements of water quality estimation for remote-sensing technology, the accuracy of PC retrieval model is more acceptable than the NC retrieval mode's.
3) The NC and PC were estimated from Landsat/TM imagery, collected from 28 October, 2003. According to the retrieval results, it was found that the distribution of NC was similar to PC, namely, higher in the south, east and center of the lake and lower in the west and north of the lake. The PC and NC varied between 0.08 mg/l and 0.12 mg/l with an average of 0.09 mg/l and between 1.84 mg/l and 2.22 mg/l with an average of 1.99 mg/l, respectively. By comparison, the NC and PC were greatly overestimated by the remote-sensing approach. The problems can be divided mainly into two groups: (a) the low accuracy of the retrieval model, and (b) the influence of atmospheric correction.
4) A lot of literatures[4], [9], [44]–[46] have proved that the NC and PC could influence the water quality concentration of chl-a, SSC and CDOM, and then, changed the optical properties of water columns. It was well known that the water color remote sensing was mainly used to detect optical properties varied with the changes of the water quality parameters, such as chl-a, CDOM, SSC and so on [37], [47]. As a result, it was feasible to estimate the NC and PC from remote-sensing data, such as Landsat/TM imagery, as long as the NC and PC were strongly related with the water quality concentration. Although it was a special case study of this paper, the modeling procedures of NC and PC estimation algorithms could give us the implication when we used the remote-sensing technology to estimate the NC and PC from similar or dissimilar aquatic environments.

References

[1] C. Giardino, M. Pepe, P. A. Brivio, P. Ghezzi, and E. Zilioli, "Detecting chlorophyll, Secchi disk, depth and surface temperature in a sub-alpine lake using Landsat imagery," *Science of the Total Environment*, vol. 268, pp. 19–29, 2001.

[2] E. V. Dafner, M. A. Mallin, J. J. Souza, H. A. Wells, and D. C. Parsons, "Nitrogen and phosphorus species in the coastal and shelf waters of Southeastern North Carolina, Mid-Atlantic U.S," *Coastal Maritime Chemistry*, vol. 103, pp. 289–303, 2007.

[3] J. Domagalski, C. Lin, Y. Luo, J. Kang, S. M. Wang, L. R. Brown, and M. D. Munn, "Eutrophication study at the Panjiakou-Daheiting Reservoir system, northern Hebei Province, People's Republic of China: Chlorophyll-a model and sources of phosphrus and nitrogen," *Agricultural Water Management*, vol. 94, pp. 43–53, 2007.

[4] A. Aminot and R. Kerouel, "An automated photo-oxidation method for the determination of dissolved organic phosphorus in marine and fresh water," *Aquatic Ecology*, vol. 76, pp. 113–126, 2001.

[5] L. Serrano, J. Penuelas, and S. L. Ustin, "Remote sensing of nitrogen and lignin in Mediteranean vegetation from AVRIS data: Decomposing biochemical from structural signals," *Remote Sens. Environ.*, vol. 81, pp. 355–364, 2002.

[6] R. E. E. Jongschaap and R. Booij, "Spectral measurements at different spatial scales in potato: Relating leaf, plant and canopy nitrogen status," *Int. J. Appl. Earth Observ. Geoinform.*, vol. 5, pp. 205–218, 2004.

[7] K. Oki and Y. Yasuoka, "Mapping the potential annual total nitrogen load in the river basins of Japan with remote-sensing imagery," *Remote Sens. Environ.*, vol. 112, pp. 3091–3098, 2008.

[8] B. B. Sridhar, R. K. Vincent, J. D. Witter, and A. L. Spongberg, "Mapping the total phosphorus concentration of biosolid amended surface soils using Landsat/TM data," *Science of the Total Environment*, vol. 407, no. 8, pp. 2894–2899, 2009.

[9] R. R. Hood, A. Subramaniam, L. R. May, E. J. Carpenter, and D. G. Capone, "Remote estimate of nitrogen fixation by Trichodesmium," *Deep-Sea Research II*, vol. 49, pp. 123–147, 2002.

[10] C. E. Hanson, A. M. Waite, P. A. Thompson, and C. B. Pattiaratchi, "Phytoplankton community structure and nitrogen nutrition in Leeuwin Current and coastal waters of the Gascoyne region of Western Australia," *Deep-Sea Research II*, vol. 54, pp. 902–924, 2007.

[11] V. Edwards, J. Icely, A. Newton, and R. Webster, "The yield of chlorophyll from nitrogen: A comparison between the shallow Ria Formosa lagoon and the deep oceanic conditions at Sagres along the southern coast of Portugal," *Estuarine, Coastal and Shelf Science*, vol. 62, pp. 391–403, 2005.

[12] R. M. Cavalli, G. Laneve, L. Fusilli, S. Pignatti, and F. Santini, "Remote sensing water observation for supporting Lake Victoria weed management," *J. Environment Management*, vol. 90, pp. 2199–2211, 2009.
[13] D. G. Hadjimitsis, C. Clayton, and L. Toulios, "Retrieving visibility values using satellite remote sensing data," *Physics and Chemistry of the Earth*, vol. 35, pp. 121–124, 2010.
[14] V. Volpe, S. Silvestri, and M. Marani, "Remote-sensing retrieval of suspended sediment concentration in shallow waters," *Remote Sens. Environ.*, vol. 115, pp. 44–54, 2011.
[15] J. Y. Wang, H. W. Zhang, and R. F. Huang, "Expression analysis of low temperature responsive genes in Eupatorium Adenophorum Spreng using cDNA-AFLP," *Plant Molecular Biology*, vol. 25, pp. 37–44, 2007.
[16] M. Onderka and P. Pekarova, "Retrieval of suspended particulate matter concentrations in the Danube River from Landsat ETM data," *Science of The Total Environment*, vol. 397, pp. 238–243, 2008.
[17] Y. Oyama, B. Matsushita, T. Fulkushima, K. Matsushige, and A. Imai, "Application of spectral decomposition algorithm for mapping water quality in a turbid lake (Lake Kasumigaura, Japan) from Landsat TM data," *ISPRS J. Photogramm. Remote Sens.*, vol. 64, pp. 73–85, 2009.
[18] Q. J. Xu, B. Q. Qin, W. M. Chen, and G. Gao, "Ecological simulation of algae growth in Taihu Lake," *J. Lakes Science*, vol. 13, no. 2, pp. 149–157, 2001.
[19] J. Chen, G. H. Zhou, J. G. Wen, and J. Fu, "Effect of remotely sensed data errors on the retrieving accuracy of territorial parameters," *Spectroscopy and Spectral Analysis*, vol. 30, no. 5, pp. 1347–1350, 2010.
[20] ASD,, Analytic Spectral Devices, Inc., Technical Guide, 3rd, 1999.
[21] J. L. Mueller and G. S. Fargion, "Ocean optics protocols for satellite ocean color sensor validation," *SeaWiFS Technical Report Series, Revision 3 Part II*, pp. 171–179, 2002.
[22] W. G. Crumpton, T. M. Isenhart, and P. D. Mitchell, "Nitrate and organic N analyses with second-derivative spectroscopy," *Limnol. Oceanogr.*, vol. 37, pp. 907–913, 1992.
[23] E. E. Prepas and F. A. Rigler, "Improvements in qualifying the phosphorus concentration in lake water," *Can. J. Fish Aquatic Sci.*, vol. 39, pp. 822–829, 1982.
[24] R. M. Chomko and H. R. Gordon, "Atmospheric correction of ocean color imagery: Using of the Junge power-law aerosol size distribution with variable refractive index to handle aerosol absorption," *Appl. Opt.*, vol. 37, no. 24, pp. 5560–5572, 1998.
[25] K. Y. Ding and H. R. Gordon, "Atmospheric correction of ocean-color sensors: Effects of the earth's curvature," *Appl. Opt.*, vol. 33, no. 30, pp. 7096–7106, 1994.
[26] W. J. Zhao, M. Tamura, and H. Takahashi, "Atmospheric and spectral corrections for estimating surface albedo from satellite data using 6S code," *Remote Sens. Environ.*, vol. 76, pp. 202–212, 2000.
[27] H. R. Gordon and D. J. Castano, "Aerosol analysis with the coastal zone color scanner: A simple method for including multiple scattering effects," *Appl. Opt.*, vol. 28, no. 7, pp. 1320–1328, 1989.
[28] H. R. Gordon and D. K. Clark, "Clear water radiance for atmospheric correction of coastal zone color scanner imagery," *Appl. Opt.*, vol. 20, no. 24, pp. 4175–4180, 1981.
[29] A. G. Dekker, R. J. Vos, and S. W. M. Peters, "Analytical algorithms for lake water TSM estimation for retrospective analysis of TM and SPOT sensor data," *Int. J. Remote Sens.*, vol. 23, pp. 15–35, 2002.
[30] J. Chen, J. Fu, and M. W. Zhang, "An atmospheric correction algorithm for Landsat/TM imagery basing on inverse distance spatial interpolation algorithm: A case study in Taihu Lake," *J. Sel. Appl. Earth Observ. Remote Sens.*, 2011, 10.1109/JSTARS.2011.2150200.
[31] P. Tett, L. Gilpin, H. Svendsen, C. P. Erlandsson, U. Larsson, S. Kratzer, E. Fouilland, C. Janzen, J. Y. Lee, C. Grenz, A. Newton, J. G. Ferreira, T. Fernandes, and S. Scory, "Eutrophication and some European waters of restricted exchange," *Continental Shelf Research*, vol. 23, pp. 1635–1672, 2003.
[32] R. J. Gowen, P. Tett, and K. J. Jones, "Predicting marine eutrophication: The yield of chlorophyll from nitrogen in Scottish coastal waters," *Marine Ecological Progress*, vol. 85, pp. 153–161, 1992.
[33] R. P. Bukata, J. H. Jerome, K. Y. Kondratyev, and D. V. Pozdnyakov, *Optical Properties and Remote-sensing of Inland and Coastal Waters*. New York: CRC Press, 1995.
[34] J. Chen, W. T. Quan, and J. H. Sun, "Relationship between nitrogen, phosphorus concentration and water quality factors," *China Envoronment Monitorinh*, vol. 21, pp. 78–82, 2011.
[35] Y. L. Zhang, B. Zhang, X. L. Wang, S. Feng, and Q. H. Zhao, "A study of absorption characteristics of chromophoric dissolved organic matter and particles in Lake Taihu, China," *Hydrobiologia*, vol. 592, pp. 105–120, 2007.
[36] S. J. Zhai, W. P. Hu, and Z. C. Zhu, "Ecological impacts of water transfers on Lake Taihu fromYangtze river, China," *Ecol. Eng.*, vol. 36, no. 4, pp. 406–420, 2010.
[37] A. Morel and S. Maritorena, "Bio-optical properties of oceanic waters: A reappraisal," *J. Geophys. Res.*, vol. 16, no. C4, pp. 7163–7180, 2001.
[38] T. R. Scott and D. C. Mason, "Data assimulation for a coastal area morphodynamic model: Morecambe Bay," *Coastal Eng.*, vol. 54, no. 2, pp. 91–109, 2007.
[39] H. Jiang, M. J. Apps, Y. Zhang, C. Peng, and P. M. Woodard, "Modelling the spatial pattern of net primary productivity in Chinese forest," *Ecological Modelling*, vol. 122, pp. 275–288, 1999.
[40] A. G. P. Dekker and S. W. M. eters, "The use of the thematic mapper for the analysis of eutrophic lakes: A case study in the Netherlands," *Int. J. Remote Sens.*, vol. 14, pp. 799–821, 1993.
[41] P. B. Robert, S. Alexander, and Y. K. Kirill, *Optical Properties and Remote Sensing of Inland and Coastal Waters*, 1st ed. New York: CRC Press, 1995.
[42] C. D. T. Vries, T. Danaher, R. Denham, R. Scarth, and S. Phinn, "An operational radiometric calibration procedure for the Landsat sensors based on pseudo-invariant target sites," *Remote Sens. Environ.*, vol. 107, pp. 414–429, 2007.
[43] J. Chen, J. Fu, and M. W> Zhang, "An atmospheric correction algorithm for Landsat/TM imagery basing on inverse distance spatial interpolation algorithm: A case study in Taihu Lake," *J. Sel. Topics Appl. Earth Observ. Remote Sens.*, vol. 4, 2011, 10.1109/JSTARS.2011.2154300.
[44] G. Hanrahan, M. Gledhill, W. A. House, and P. J. Worsfold, "Evaluation of phosphorus concentrations in relation to annual and seasonal physico-chemical water quality parameters in a UK chalk stream," *Water Research*, vol. 37, pp. 3579–3589, 2003.
[45] J. E. Ruley and K. A. Rush, "Development of a simplified phosphorus management model for a shallow, subtropical, urban hypereutrophic lake," *Ecol. Eng.*, vol. 22, 2004.
[46] Y. Liang, J. Beardall, and P. Heraud, "Effects of nitrogen source and UV radiation on the growth chlorophyll fluorescence and fatty acid composition of Phaeodactylum tricornutum and Chaetoceros muelleri (Bacillariophyceae)," *J. Photochem. Photobiol.*, vol. 82, pp. 161–172, 2006.
[47] C. D. Mobley, L. K. Sundman, and E. Boss, "Phase function effects on oceanic light fields," *Appl. Opt.*, vol. 41, no. 6, pp. 1035–1050, 2002.

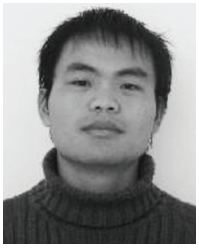

Jun Chen graduated from China University of Petroleum, China, in 2005. He received the M.A. degree in geography in 2009 from the China University of Geosciences, China.

He is currently an Associate Professor in the Qingdao Institute of Marine Geology of Ministry of Land and Resources of the People's Republic of China. His primary research interests are in environmental remote sensing.

Wenting Quan, photograph and biography not available at the time of publication.